Egypt. J. Chem. **Vol. 68,** No. 10 pp. 493 - 509 (2025)

Egyptian Journal of Chemistry

http://ejchem.journals.ekb.eg/

Characterization and Potentiality of Calcined Kaolins for Metakaolin Production

Yasmen G Abdel-Maksoud*[1], Mohamed M Abu-Zeid[1], Fawzia Abd EL-Raoof[2], AbdelMonem M Soltan[1], Mahmoud M Hazem[3]

1 Geology Department, Faculty of Science, Ain Shams University, 11566, Cairo, Egypt
2 Refractories, Ceramic, and Building Materials Department, National Research Centre, 12311 Dokki, Cairo, Egypt
3 Chemistry Department, Faculty of Science, Ain Shams University, 11566, Cairo, Egypt

Abstract

This study aims to optimize the calcination conditions of Egyptian kaolins to produce metakaolin as pozzolanic material. Technological samples were collected from the kaolin quarries at Sinai, Egypt. The kaolin and metakaolin samples were characterized using laser size analysis, XRD, IR, XRF, TG, SEM and BET. The results showed that 66% of the fired samples are of highly pozzolanic activity (≥700mg $Ca(OH)_2$/g metakaolin). The optimum pozzolanic activity (1732mg $Ca(OH)_2$/g metakaolin) is given after kaolin calcination at 550°C for 30mins due mainly to the high kaolinite/quartz ratio as well as the low total fluxes content of the raw kaolin samples. The fluxes promote the agglomeration of the metakaolin particles during calcination causing the decrease of the metakaolin surface area and consequently minimize the reactive sites available for reaction. The optimum metakaolin at 550°C for 30mins has a maximum surface area and low pore volume of 13.99 m^2/g and 0.116 cm^3/g, respectively. This is attributed to the fact that the smaller pores provide higher surface area per unit volume of the metakaolin. The optimization of kaolin calcination conditions has add-values for the industrial upscaling of kaolin into metakaolin.

keywords: Kaolin, Calcination, Metakaolin, Reactivity

1. Introduction

Egypt is the first kaolin producer in Africa and the Middle East, ranking 19th worldwide [1]. In the last decade, the total production of Egyptian kaolin is approximately 3,702,000 metric tons with an average of 375,000 metric tons per year representing 1% of the worldwide production [2, 3]. The significant economic kaolin reserves in Egypt are located at southwestern Sinai (Abu Zenima), Red Sea (Abu Darag) and southwest Aswan (Wadi Kalabsha) [4–9]. According to Abd El Razek [10], the highest quality among all the Egyptian kaolin is recorded in Abu Zenima, at 120 million tons of grades ranging from 26% to 35% Al_2O_3 [11]. Kaolin is enriched with the mineral kaolinite ($Al_2(OH)_4SiO_2$) [12–14] that is thermally activated to produce metakaolin (MK)($Al_2SiO_2O_2$) that is a highly reactive pozzolanic material. Rather than thermal activation, MK could be generated by mechanical and chemical activation of raw kaolin. Thermal activation methods involve resistant heating in rotary kilns whereas the mechanical methods rely on prolonged grinding, however the chemical methods depend on the usage of activators such as acid or alkaline compounds to activate the raw kaolin into metakaolin [15]. MK pozzolanic activity depends mainly on its amorphous nature that plays an important role in the strength performance of alkali activated binders (AABs) [16]. The kaolin calcination temperature affects produced metakaolin the reactivity of the produced MK.

Many researchers studied the effects of the calcination temperature on the pozzolanic reactivity of MK [17–20, 23, 68, 74]. Shafiq *et al.* [21] and Eldin *et al.* [75] reported that the final properties of the calcined kaolin depend on the processing conditions, including calcination temperature, rate and holding time. Hollanders *et al.* [22] calcined clay samples (4 kaolinitic, 3 smectitic and 1 illitic) in a fixed-bed electrical furnace at temperatures ranging between 500 and 900°C. The results indicated that all kaolinitic clays are highly reactive at a broad range of firing temperatures (500-900°C).

The kaolinite degree of ordering, as the main mineral in the raw kaolin, influences the optimal activation temperature and the rate of the calcined kaolin-lime reaction. Kassa *et al.* [23] concluded that the MK pozzolanic activity is linearly increased with the calcination temperature until 700°C and showed a maximal value of 1235mg $Ca(OH)_2$ g^{-1}. It was found that the pozzolanic activity is significantly reduced from 1235 to 445mg $Ca(OH)_2$ g^{-1} at the temperature range 700-1000°C. This decline in pozzolanic activity might be occurred above 700°C due to the agglomeration of MK and formation of spinel phase. Onyelowe *et al.* [24] reported that the MKs after calcination at 550°C and 800°C have the optimum pozzolanic potentials of 96.26% and 96.28%, respectively. The pozzolanic potential increases at optimal calcination due to the higher specific surface area of metakaolin.

The pozzolanic reactivity is affected by the chemical and mineralogical characteristics of raw kaolin and the calcination process. The properties of raw kaolin include kaolinite content and degree of crystallinity while the calcination process controls the degree of de-hydroxylation and particle size distribution [20, 25–29, 69]. Metakaolin is appropriate for use as: i) ecological pozzolanic additive for ordinary Portland cement (OPC), ii) precursor of geopolymers, iii) carrier/supplier of metal nanoparticles

*Corresponding author e-mail: y.gamal1992@yahoo.com-yasmingamal@sci.asu.edu.eg.; (Yasmen G Abdel-Maksoud).
Receive Date: 06 February 2025, Revise Date: 03 March 2025, Accept Date: 07 March 2025
DOI: 10.21608/ejchem.2025.358543.11269

with bactericidal/virucidal activity, and iv) catalytic reactions [14]. This work focused on the characterization of kaolin quarried technological samples from El-Garf area, Abu Zenima, before and post calcination. This will add-value for the kaolin up-scaling, as a raw material, into metakaolin at optimum calcination conditions.

2. Materials and Methods

2.1. *Materials*

Serial samples were collected from three kaolin quarries at El-Garf area in Abu Zenima southwestern Sinai. The representative technological kaolin samples (Ga1-Ga5) were crushed using Jaw Crusher then ground by Pulverisette 6 of Fritsch Co., Germany. The ground samples were sieved <63µm then subjected to detailed analysis.

2.2. Methods

2.2.1. Chemical Attack

The kaolin samples were chemically attacked by diluted hydrogen chloride (HCl 10%), hydrogen peroxide (H_2O_2 10%) and oxalic acid ($C_2H_2O_4$, 5%) to quantify the total carbonate, organic matter and free iron oxide contents that bind the kaolin samples mineral grains (Table 1) [30–32].

2.2.1. Grain Size Analysis

The particle size distribution of the studied technological samples was determined using the laser size technique CILAS 1064 Naß.

2.2.2. X-Ray Diffraction Analysis (XRD)

X-ray diffraction analysis was used to determine the mineral compositions of the bulk raw kaolin samples by using D8 Discover, Bruker Co. Germany with Cu-target tube and Ni filter at 40kV, 40Ma, wavelength 1.54A and a scanning speed of 0.02°/sec. The diffraction peaks in the range $2\theta = 2 - 75^{o}$, d-spacings and relative intensities (I/I^{o}) were recorded and compared with the standard data published by the American Society for Testing and Materials (ASTM) and Match software. This instrument is connected to a computer system using X-40 diffraction program and ASTM data for mineral identification.

2.2.3. Determination of Organic Matter (FTIR)

The kaolin samples were investigated by Infrared spectroscopic analysis (IR) using Bruker Vertex 80, optical resolution of <0.06 cm^{-1} and a wide spectral range for the room temperature Dlatgs detector (12,000 to 20 cm^{-1}). The wave number of infrared spectra is ranging from 400 to 4000 cm^{-1}.

2.2.4. Chemical Composition (XRF)

The chemical composition of the samples was determined using X-ray fluorescence (XRF) with the spectrometer Axios advanced, Sequential WD-XRF Spectrometer, Panalytical 2005.

2.2.5. Thermal Behavior (TGA-DTG)

The thermal behavior of the kaolin samples was determined using TGA 50 thermal analyzer (Schimadzu Co. Tokyo, Japan) with a heating rate of 25°/min up to 1000 °C under dynamic nitrogen atmosphere.

2.2.6. Microstructure (SEM)

The detailed microstructure of the raw kaolin before and after calcination was investigated by the scanning electron microscope (SEM) using Quanta FEG 250. Before SEM investigation, the selected samples were soaked for 30 minutes in Ethyle alcohol in an ultrasonic cleaner (Elmasonic) then dried in a Heratherm oven overnight before scanning.

2.2.7. Pozzolanic Activity

The five technological kaolin samples were calcined in a bottom loading electrical Nabertherm muffle. The applied calcination conditions were in the range 550 to 850°C with a heating rate of 5°C/min and soaking times of 30, 60 and 120mins. The selected temperature range is justified by the fact that kaolinite, which is the main mineral in kaolin, begins to dissociate around 550°C and to sinter at 850°C. The calcination of the kaolin samples was achieved at different soaking times to optimize the prolongation of the samples heat treatment. The calcined samples were then suddenly cooled, i.e., air quenched, where a total of 60 calcination trials were conducted on the kaolin samples to produce MK.

After calcination, the pozzolanic activity of the calcined kaolins, i.e., metakaolins (MKs) were assessed using the modified Chapelle test according to the NF P18-513 standard. This test allows the quantification of $Ca(OH)_2$ fixed (consumed) by 1g of MK when mixed with 2g of CaO and 250ml of distilled CO_2 free water. Each sample suspension then was boiled with continuous stirring at 80°C for 16hrs in a 500ml stainless steel Erlenmeyer. After boiling, the Erlenmeyer was cooled to ambient temperature with tap water. The portlandite ($Ca(OH_2)$) content that was not consumed (free in solution) was determined by sucrose extraction and acid titration. This was achieved by adding 250ml of fresh sucrose solution (0.7M) to the solution and stirring with a magnetic bar for 15mins. A 200ml of the final solution were filtrated, and 25ml was titrated with HCl 0.1N using 2-3 drops of phenolphthalein (0.1w/v% in ethanol 50v/v%). The titration reactions are:

$$CaO+2HCl \rightarrow CaCl_2+H_2O \text{ (Eq. 1)}$$

$$Ca(OH)_2 + 2HCl \rightarrow CaCl_2 + 2H_2O \text{ (Eq. 2)}$$

The average pozzolanic activity of MK was calculated (Eq. 3), after three experimental trials for measurements.

$$PAM=2(V1-V2/V1)*(74/56)*1000 \text{ (Eq. 3)}$$

Where:
PAM: pozzolanic activity of metakaolin expressed in mg $Ca(OH)_2$ fixed / g metakaolin.
V1: volume (ml) of HCl 0.1N, necessary for titrating 25ml of the final solution obtained without metakaolin (blank test).
V2: volume (ml) of HCl 0.1N, necessary for titrating 25ml of the final solution obtained with metakaolin.
The blank test (without metakaolin) must verify V1*56/2 < 1000.

2.2.8. Surface Area and Pore Size (BET)

The Brunauer-Emmett-Teller (BET) method was applied to measure the surface area and pore size distribution of kaolin and MK samples. The adsorption-desorption of N_2 gas at -196°C (77K) using Automatic surface area and pore size analyzer (BELSORP MINI X) was measured.

3. Results and Discussion

3.1. Kaolin Characterization

3.1.1. Chemical Attack and Particle Size Distribution

After the chemical attack of the kaolin samples, it was found that the total carbonate, organic matter and free iron contents, that bind the kaolinite flakes, lie in the ranges (0.07-2.50), (0.10-0.90) and (0.22-3.43wt.%), respectively (Table 1). Following to the chemical attack, the samples had been prepared for particle size distribution applying the laser diffraction method. The grain size distribution of El-Garf kaolin samples (Ga1-Ga5) shows that the cumulative less than D10, D50 and D90 are in the ranges (0.60-2.20), (6.60-25.00) and (30.00-56.00µm), respectively, revealing the samples to be nominated as ¨coarse silt¨ except for sample (Ga3) ¨medium silt¨ (Fig. 1).

Table 1: Compositional and textural characteristics of the kaolin technological samples

Locality	Sample code	Carbonate	Organic matter	Iron oxides	D10	D50	D90	Nomenclature, (Folk, [78])
			(wt.%)			(µm)		
El-Garf	**Ga1**	0.95	0.75	0.22	2.20	25.00	56.00	Coarse silt
	Ga2	0.45	0.90	2.19	0.90	11.00	38.00	Coarse silt
	Ga3	2.50	0.10	0.40	0.90	7.50	30.00	Medium silt
	Ga4	0.10	0.66	3.43	0.60	6.60	34.00	Coarse silt
	Ga5	0.07	0.12	1.84	1.00	15.00	36.00	Coarse silt
	Average	**0.81**	**0.51**	**1.62**	**1.12**	**13.02**	**38.80**	

Note* Ga1-Ga5: Raw kaolin samples D10, D50 and D90: The grain diameter of 10, 50 and 90vol.%

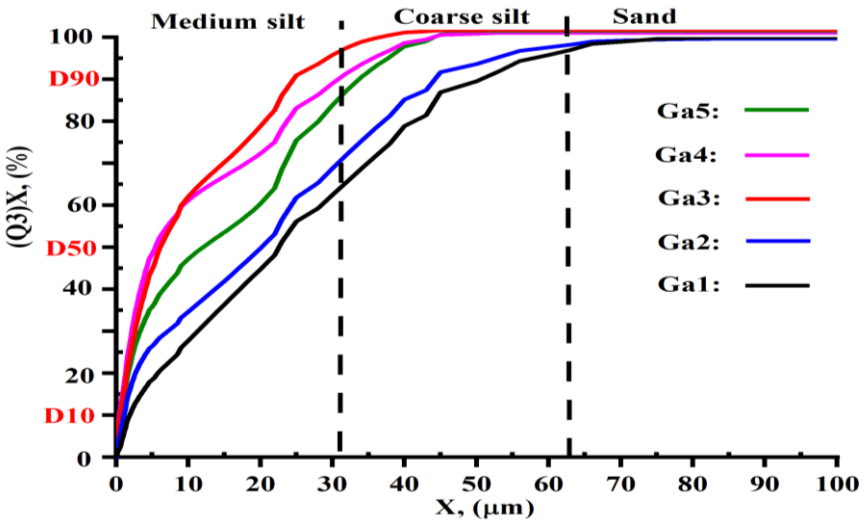

Fig. 1. Grain-size distributions of the kaolin samples (Ga1-Ga5) of El-Garf locality.

3.1.2. Mineral Composition

The phase composition of El-Graf kaolin samples was determined using XRD. The bulk as well as the oriented, heated and glycolated kaolin slides were investigated to identify the non-clay and clay minerals, respectively. The main non-clay minerals are quartz (Q, "SiO_2", PDF# 05-0490) and anatase (A, "TiO_2", PDF# 84-1286) in all samples (Fig. 2). Kaolinite (K; "$2SiO_2.Al_2O_3.2H_2O$", PDF# 14-0164) is the only recorded clay mineral as confirmed from the disappearance of its main peaks at ~7.10 and 3.56 Å of the heated samples (Figs. 3a-e).

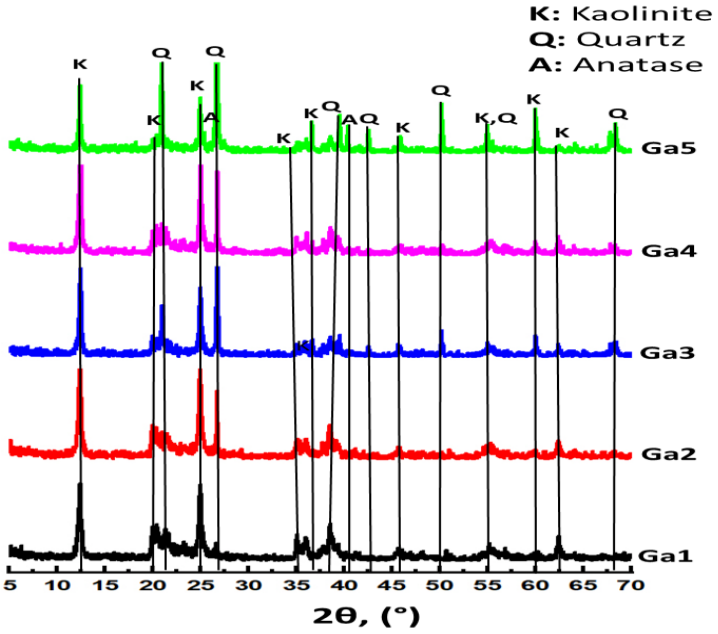

Fig. 2. XRD diffractograms of the bulk kaolin samples from El-Garf (Ga).

3.1.3. FTIR Spectroscopy

The IR absorption spectra are shown in figure (4). The kaolinite absorption bands for the O-H, Si-O, Si-O-Si, O-H-Al and Si-O-Al^{VI} function groups are shown in the ranges 3620-3700; 910-1120; 420-466; 915 and 540cm^{-1}, respectively [28, 33–37]. In addition, the organic matter is confirmed by the presence of the spectral bands for the alcohol (O-H), alkanes (sp^3 C-H) and alkyne (C≡C) at 3775-3787; 2850-3000 and 2142-2373cm^{-1}, respectively, in all samples [38–40]. The latter organic matter function groups are in conformity with the organic matter contents that determined by the H_2O_2 chemical attack (Table 1).

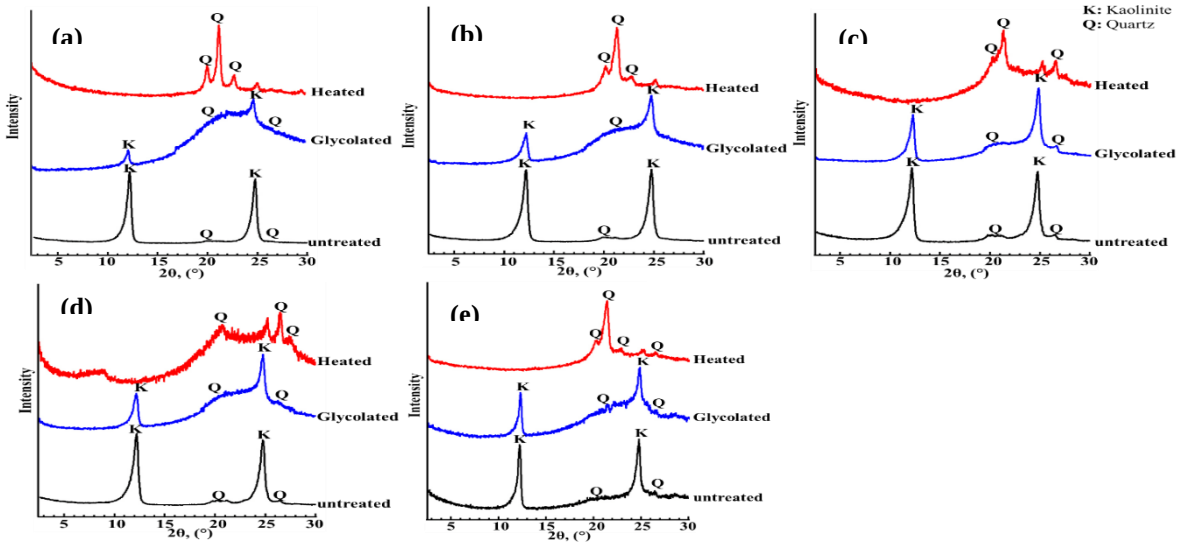

Fig. 3. X-ray diffractograms of the clay fractions of El Garf samples: (a) Ga1, (b) Ga2, (c) Ga3, (d) Ga4 and (e) Ga5.

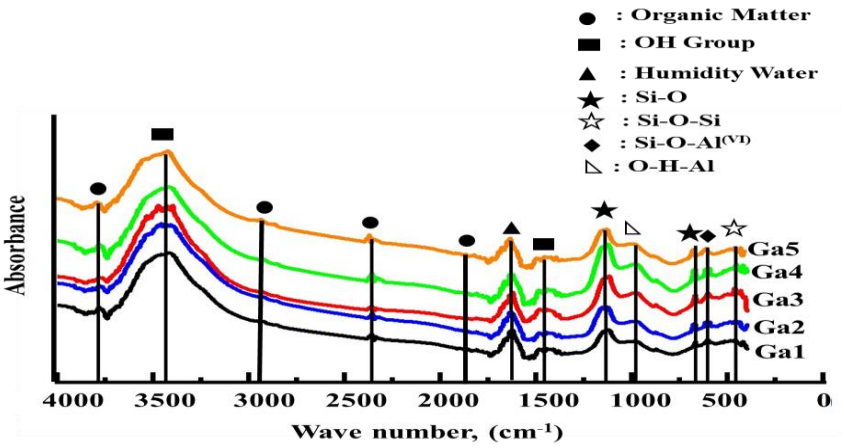

Fig. 4. FT-IR spectra of raw kaolin samples from El-Garf samples (Ga).

3.1.4. Chemical Constitution

The chemical composition of the kaolin samples is shown in Table (2). The SiO_2 content (45.19-68.87; average 52.78wt.%) (Table 2) is mainly sourced from the tetrahedral silica sheets of the kaolinite minerals as well as the free quartz grains that are disseminated among the kaolinite flakes. The Al_2O_3 contents lie in the range (21.21-36.74; average 31.19wt.%) where it is mainly sourced from the kaolinite. Based on the SiO_2 and Al_2O_3 of the kaolin samples, it is possible to quantify their kaolinite and quartz contents according to equations (4 and 5) [41]:

$$\mathbf{K}\ (\%) = \frac{\textbf{one mole of kaolinite} \times \textbf{alumina content from chemical analysis}}{\textbf{one mole of alumina}} \quad \text{(Eq. 4)}$$

$$\mathbf{S = S_{Ch} - S_K} \quad \text{(Eq. 5)}$$

Where: K: Kaolinite S: The excess silica presents as free quartz S_{Ch}: The chemically determined silica content S_K: The required silica for kaolinite

The calculations show that the kaolinite and quartz are averaging 78.99; 16.06wt.% in all samples whereas the former is maximized in sample Ga1 associated with the least quartz content (93.04 and 1.94wt.%, respectively). However, the situation is reversed in sample Ga5 (43.81 and 53.71wt.%, respectively). The calculated mineral contents match the SiO_2 and Al_2O_3 contents of the kaolin samples (Table 2). The relations between the kaolinite/quartz vs. the SiO_2 and Al_2O_3 contents (Table 2) show a general negative (r= 0.94) and positive (r= 0.97) correlations, respectively (Figs. 5a, b).

TiO_2 and Fe_2O_3 are the main coloring oxides (Table 2). The Fe_2O_3 contents lie in the range (1.05-2.86; average 1.84wt.%) and mainly sourced from the free iron oxides that may bind the kaolinite grains (Table 1). The maximum concentration of Fe_2O_3 (2.86wt.%) was recorded in sample Ga4 (Table 2) mainly due to its highest content of free iron oxide cements (3.43wt.%, Table 1). On the other hand, the minimum concentration (1.05wt.%) occurs in sample Ga1 (Table 2) due to its lowest content of the free iron binding material (0.22wt.%, Table 1). The TiO_2 concentrations lie in the range (1.16-2.72; average 1.84wt.%). The maximum concentration of TiO_2 (2.72wt.%) was recorded in sample Ga5 (Table 2) which is attributed mainly to its possible occurrence in the kaolinite lattice and as free titania as anatase as well (Fig. 2) [42, 43]. On the other hand, the minimum content of TiO_2 (1.16wt.%) occurs in sample Ga1 [41, 44–47].

Table 2: Chemical composition (wt.%) and Percentages of kaolinite and quartz as determined from chemical analysis data of the raw kaolin samples

Locality	Sample code	SiO_2	TiO_2	Al_2O_3	Fe_2O_3	MgO	CaO	Na_2O	K_2O	P_2O_5	SO_3	Cl	LOI	K	Q	K/Q ratio
El-Garf	**Ga1**	45.19	1.16	36.74	1.05	0.10	0.09	0.10	0.02	0.13	0.09	0.03	14.96	93.04	1.94	48.04
	Ga2	46.44	1.76	35.62	1.36	0.07	0.03	0.12	0.02	0.08	0.19	0.02	13.93	90.21	4.51	20.02
	Ga3	54.34	1.98	29.98	2.70	0.07	0.06	0.05	0.14	0.08	0.19	0.02	10.13	75.93	19.05	3.99
	Ga4	49.16	1.58	32.42	2.86	0.12	0.10	0.04	0.16	0.10	0.11	0.02	13.09	82.10	10.99	7.47
	Ga5	68.78	2.72	21.21	1.23	0.06	0.04	n.d.	0.07	0.08	0.11	0.03	5.33	53.71	43.81	1.23
	Average	**52.78**	**1.84**	**31.19**	**1.84**	**0.08**	**0.06**	**0.07**	**0.08**	**0.09**	**0.13**	**0.02**	**11.48**	**78.99**	**16.06**	**16.15**

Note* n.d.: Not detected Ga1-Ga5: Raw kaolin samples LOI: Loss on ignition K: Kaolinite Q: Quartz K/Q ratio: kaolinite/Quartz

The total contents of alkalies (Na_2O and K_2O) in the studied kaolin samples are minor (0.07-0.20, average 0.14wt.%) (Table 2) with maximum concentration (0.20wt.%) in sample Ga4 (Table 2) due to the presence of high organic matter content (0.66wt.%, Table 1) that can adsorb Na and K [73]. However, the minimum occurrence of organic matter (0.07wt.%) is recorded in sample Ga5 (Table 2) due to the presence of low organic matter content (0.12wt.%, Table 1).
The LOI values of the kaolin samples lie in the range (5.33-14.96; average 11.49wt.%) (Table 2). The maximum value (14.96wt.%) was recorded in sample Ga1 (Table 2) mainly due to its high content of kaolinite (93.0wt.%, Table 2). On the other hand, the minimum LOI value (5.33wt.%) characterizes sample Ga5 (Table 2) as it has the lowest content of kaolinite (53.71wt.%, Table 2). The LOI are directly related to the proportions of Al_2O_3 contents, i.e., kaolinite concentrations, (Table 2) with r= 0.94 (Fig. 5c) [7].

3.1.5. Thermal Dissociation

The TGA-DTG thermograms of the studied samples are presented in figure (6). Two main mass losses were determined. The first loss (0.82-1.33wt.%) is represented by the endothermic peaks in the temperature range (50.62-57.69°C) and is attributed mainly to the loss of the free moisture water [48, 49]. The second mass loss (4.38-11.49wt.%) is represented by the endothermic peaks in the temperature range (559.27- 580.37°C) that related to the de-hydroxylation of the kaolinite crystalline water and its transformation into a disordered phase, i.e., metakaolin (MK) ($Al_2Si_2O_7$) and H_2O [16, 33, 49–52]. Small exothermic peak at 722.14°C is related to the existence of the anatase in sample Ga5. The total mass losses of all kaolin samples range from 5.26 to 13.81wt.%.
The degree of kaolinite ordering was determined using the thermogravimetric data according to Smykstz [53]. If the de-hydroxylation maximum peak temperature is < 530, (530-555), (555-575), >575, the kaolinite degree of ordering is referred as “extremely disordered”, “strongly disordered”, “slightly disordered” and “well ordered”, respectively [53]. According to this classification, the kaolinite in samples Ga1, Ga2 and Ga4 are referred as “well ordered” where their decomposition peaks occur in the temperature range (577.7-580.37) whereas Ga3 and Ga5 samples are classified as “slightly disordered” due mainly to the kaolinite decomposition peaks that appear at (561.35 and 559.27°C), respectively (Fig. 6). The higher the degree of kaolinite ordering, the higher is the structural decomposition temperature [54].

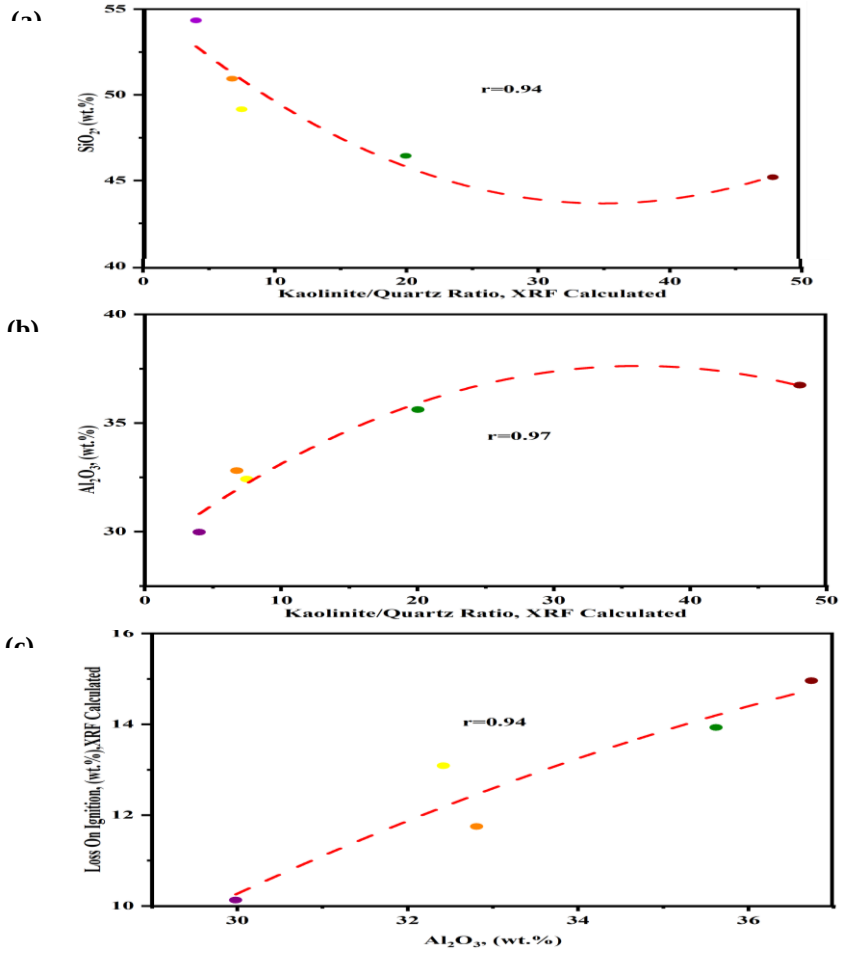

Fig. 5. Variation diagrams of (a) SiO_2 and kaolinite/quartz ratio, (b) Al_2O_3 and kaolinite/quartz ratio and (c) Al_2O_3 and kaolinite/quartz ratio where, **r:** correlation coefficient.

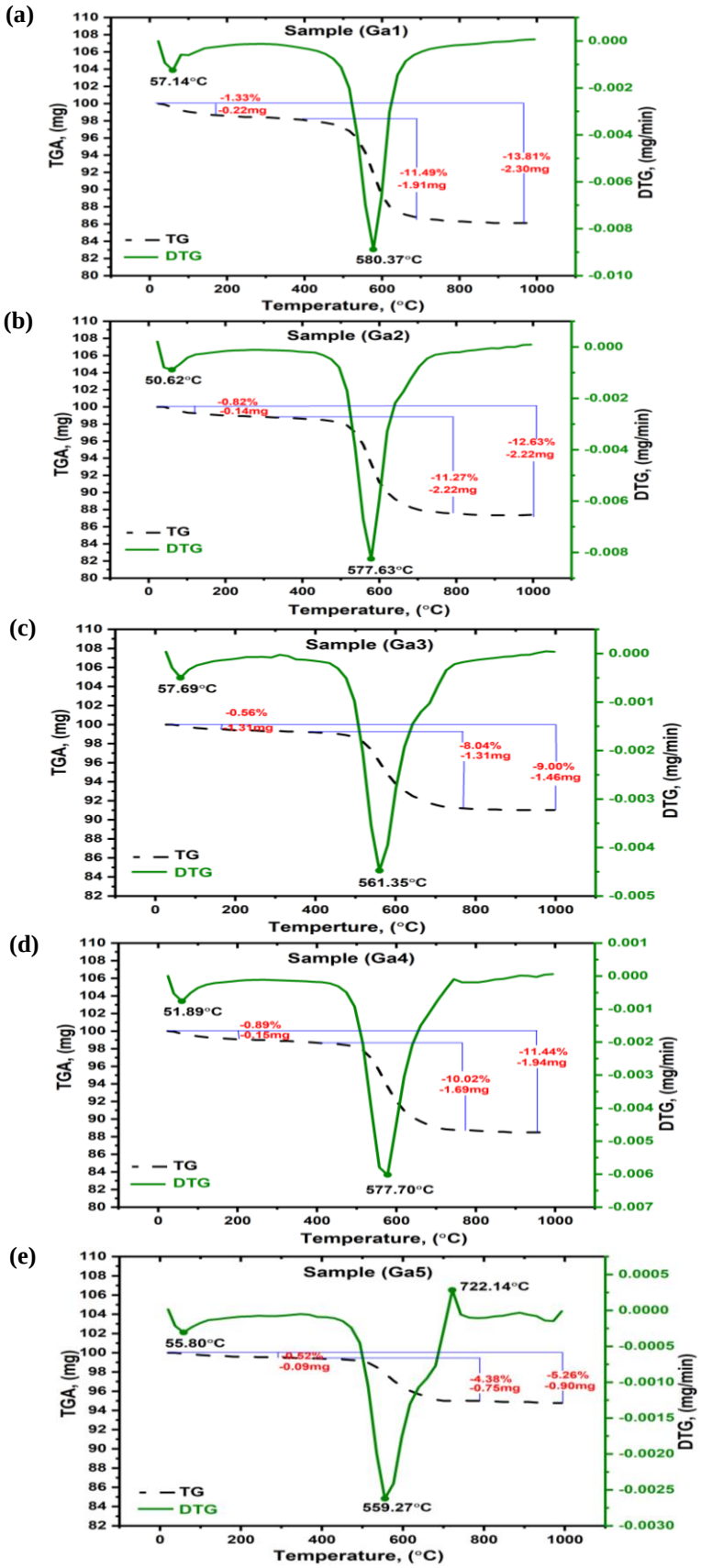

Fig. 6. TGA-DTG curves for the kaolin samples from El-Garf.

3.1.6. Microstructure

The microstructures of selected kaolin samples were examined using SEM. In sample Ga1, kaolinite exists as crystals and crystal aggregates made up of pseudo-hexagonal platelets (Fig. 7a). This mature structure is in conformity with its calculated high degree of ordering (Fig. 6a) that demanded the maximum decomposition temperature at 580.37°C with maximum weight loss (11.49wt.%) (Fig. 6a) among all the kaolin samples [34, 55–58]. However, in sample Ga5, kaolinite occurs as ragged crystal aggregates with irregular outlines (Fig. 7b). This immature texture conforms well to its calculated low degree of kaolinite ordering (Fig. 6e) demanding the minimum decomposition temperature at 559.27°C (Fig. 6e) that is lower than that recorded for sample Ga1 (580.37°C, Fig. 6a) with about 21.1°C.

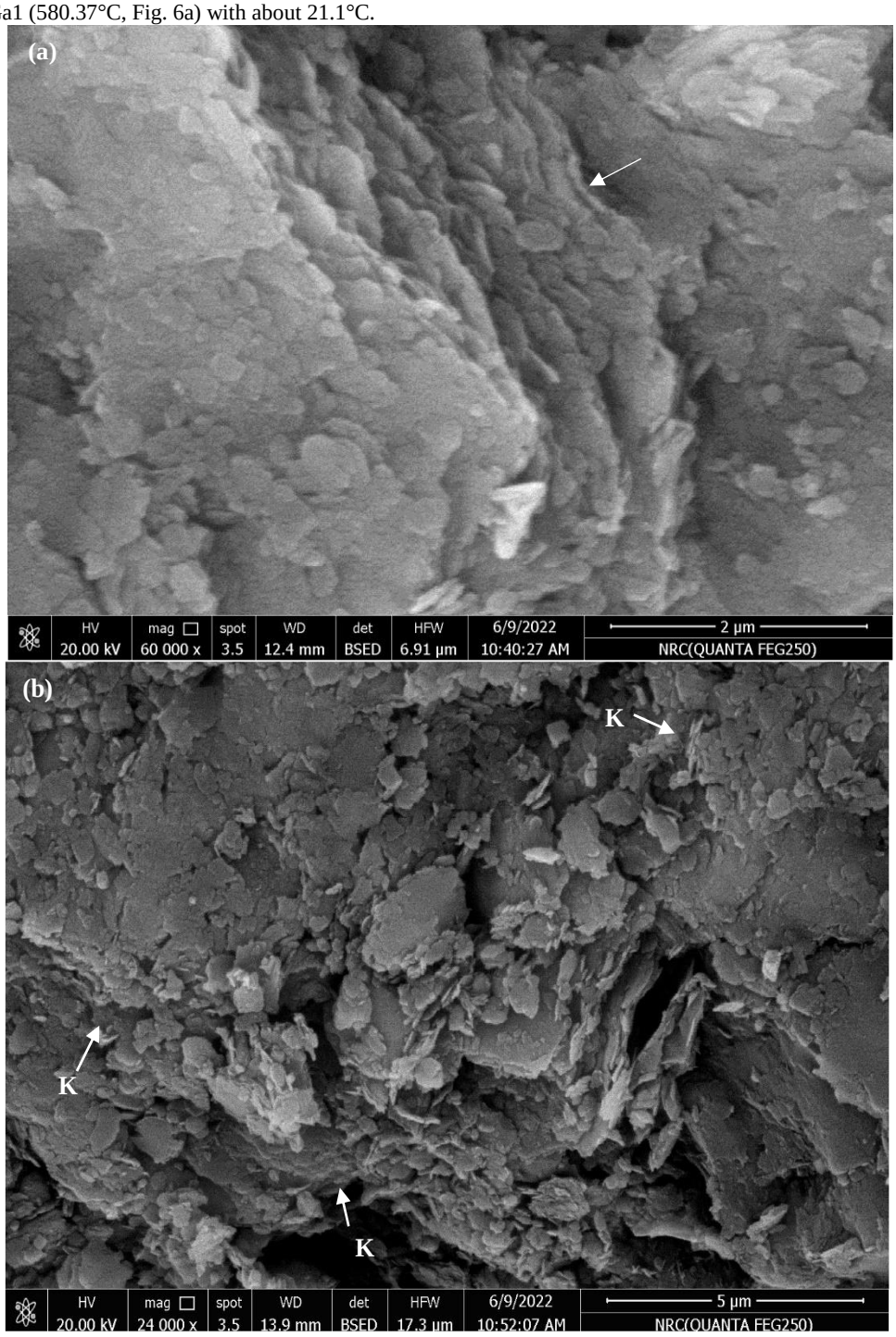

Fig. 7. BS-SEM micrographs of the kaolin samples (a) the distinctly ragged outlines of kaolinite crystal (Ga1) aggregates and (b) highly-ragged crystal aggregates of kaolinite (Ga5) (K, white arrows).

3.2. Characterization of Calcined Kaolin

3.2.1. Pozzolanic Activity of MKs

The pozzolanic activities of the MKs were measured using the modified Chapelle test according to the NF P18-513 standard [59–61]. According to the latter standard, the weight of the pozzolanic MK should not be <700mg $Ca(OH)_2$/g MK. Pozzolanic activity > 1200mg $Ca(OH)_2$ /g MK would be classified as high active pozzolan whereas the pozzolanic activity <700mg $Ca(OH)_2$/g MK would be classified as non-pozzolan [62]. The average pozzolanic activity for each MK sample after each firing trial was calculated for the average of three measurements, therefore, a total number of 180 titration trials were conducted.

Figure (8) shows the behaviour of the average pozzolanic activity for all the MKs under the applied firing conditions. It shows that the pozzolanic activity decreased with increasing the calcination temperature (550, 650, 750 and 850°C) and soaking time (30, 60 and 120min) in all samples. This could be related to the possible MKs particle agglomeration resulted from promoting the bonding between these particles at higher calcination temperature and/or time with a consequent reduction of the effectiveness of MKs dispersion (Fig. 8) [63].

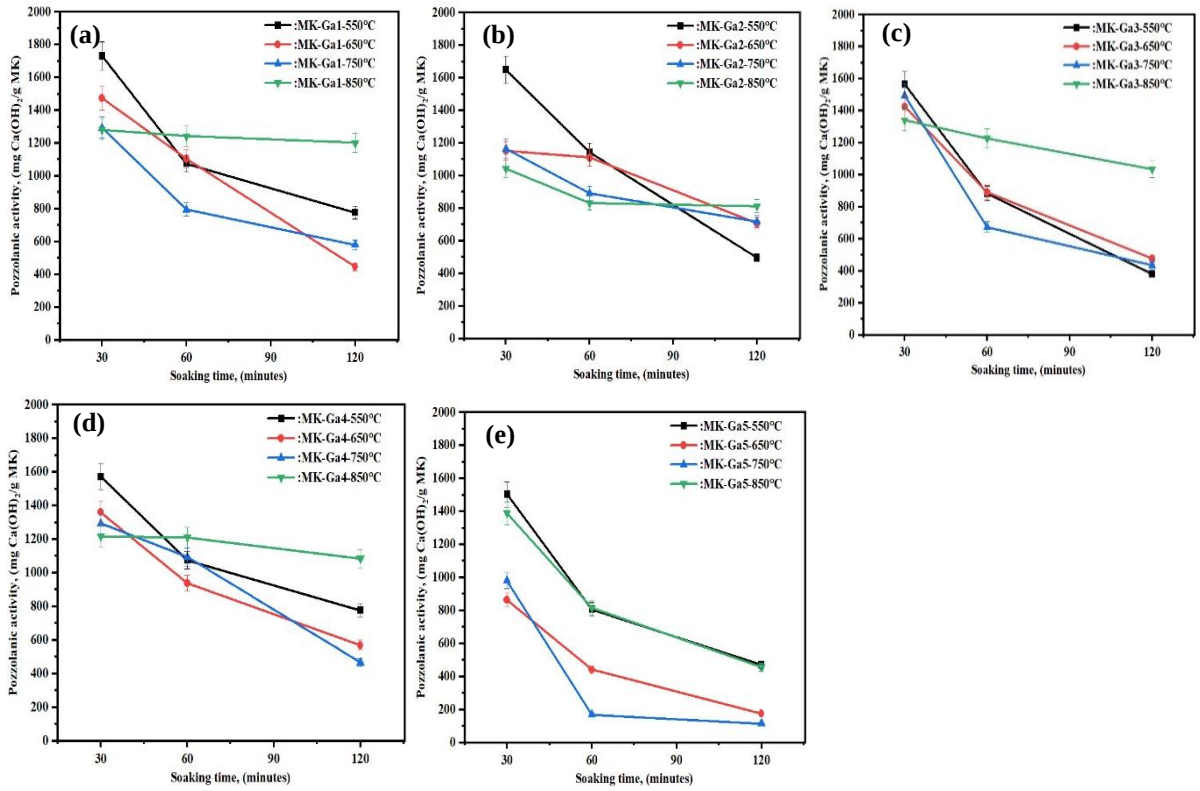

Fig. 8. The pozzolanic activities of El-Garf MKs samples: (a) Ga1, (b) Ga2, (c) Ga3, (d) Ga4 and (5) Ga5.

The maximum pozzolanic activity of sample MK-Ga1 (1732mg $Ca(OH)_2$/g MK) ¨high active pozzolan¨ after calcination at 550°C for 30mins (Fig. 8a) is attributed to its maximum content of kaolinite (93.04wt.%) when compared with that of sample Ga5 (53.71wt.%) (Table 2) that resulted in the minimum pozzolanic activity of MK-Ga5 (1504mg $Ca(OH)_2$/g MK) (Fig. 8e). In addition, as the total fluxing oxides (sum of Fe_2O_3, TiO_2, CaO, MgO, SO_3, K_2O, Na_2O and P_2O_5) of the kaolin samples affect their MKs counterpart pozzolanic activities [19, 59, 64], sample Ga5 has the maximum total fluxes (4.34) when compared with Ga1 (2.77wt.%), to explain the lower pozzolanic activity of Ga5-MK. The higher the total fluxes, the higher is the agglomeration of the MK particles [19, 59, 64].

Eldin *et al.* [75] demonstrated that some kaolins from Abu Zenima are optimally transformed into metakaolin at 700 °C for 90 minutes. The pozzolanic activity of the later metakaolin ranges from 0.65 to 0.74 g $Ca(OH)_2$/g MK. However, Khaled *et al.* [68] reported the optimum calcination of the same kaolins to be at 600 °C for 60 minutes where higher pozzolanic activity of 1156.6 mg $Ca(OH)_2$ /g MK was calculated according to the Chapelle method (NF P18-513, [76]). This study proved that the optimum calcination of Abu Zenima kaolins could be achieved at 550 °C for 30 minutes to produce MK with an even greater pozzolanic activity of 1732 mg $Ca(OH)_2$ /g MK than Eldin *et al.* [75] Khaled *et al.* [68].

The calculated pozzolanic activity proved that > 66% of the measured samples are pozzolanic, i.e., >40 firing conditions, and can be used on the industrial scale to produce highly pozzolanic MKs. On the other hand, the relationship between the pozzolanic activity vs. the kaolinite/quartz ratio indicates a general positive correlation with significant $r \geq 0.5$ (Fig. 9).

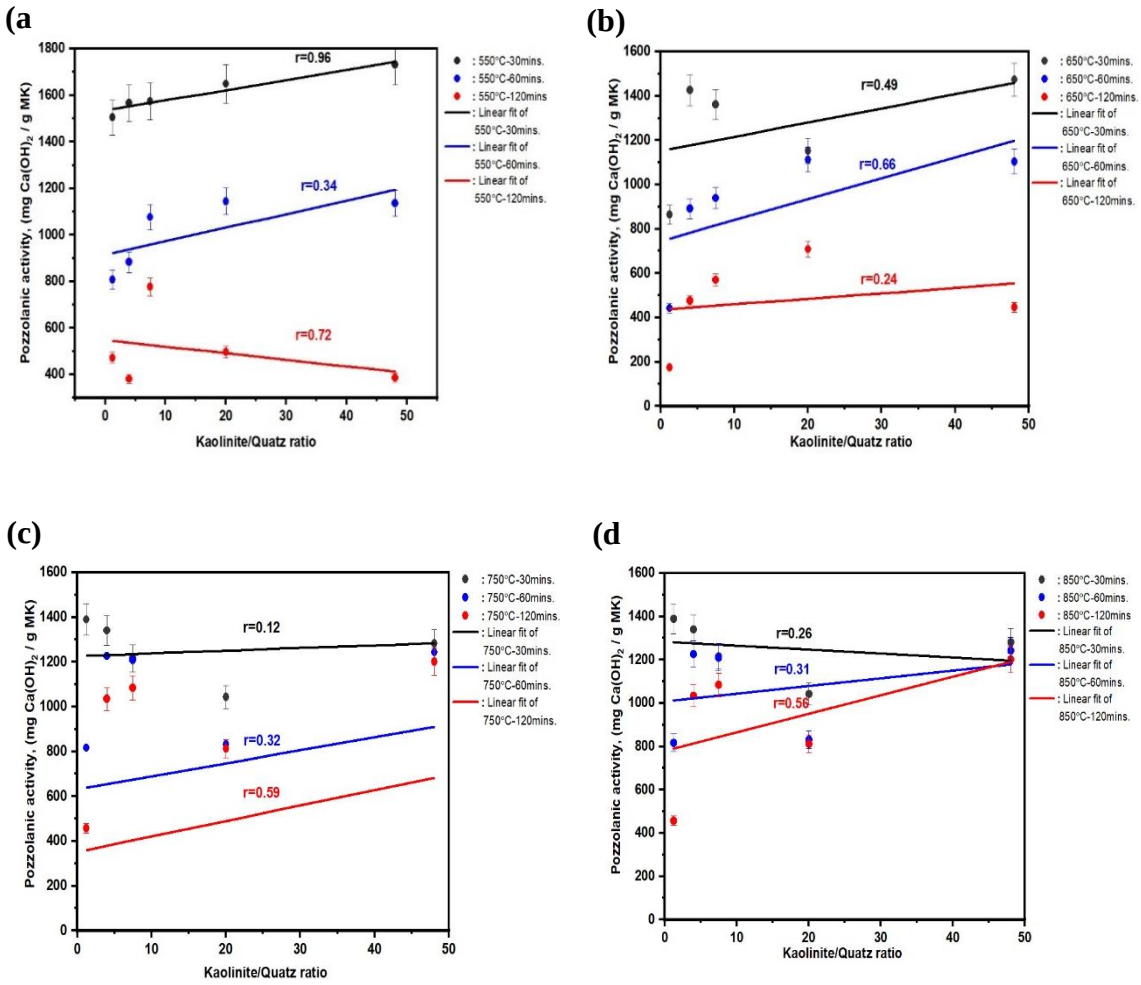

Fig. 9. The relationship between the pozzolanic activity vs. kaolinite/quartz ratio in all samples at: (a) 550, (b) 650, (c) 750 and (d) 850 for 30, 60 and 120mins; respectively where, **r:** correlation coefficient.

3.2.2. Phase Composition of MK

The XRD pattern of the MK-Ga1 sample showed a wide amorphous hump at the 2θ range (15-30°) referring to the complete decomposition, i.e., amorphization, of the kaolinite mineral contents (Fig. 10) [22, 65]. The amorphous humps are directly related to the transformation of kaolinite to MK ($2SiO_2Al_2O_3$) by the removal of the structural OH groups, rearrangement of Si and Al ions and the formation of penta- and tetra-coordinated Al ions at the expense of the hexa-coordinated Al ions (Eq. 6) (Fig. 10) [37, 56, 63, 66–69].

$$2SiO_2\ Al_2O_3\ 2H_2O \rightarrow 2SiO_2\ Al_2O_3 + 2H_2O \qquad \text{(Eq. 6)}$$

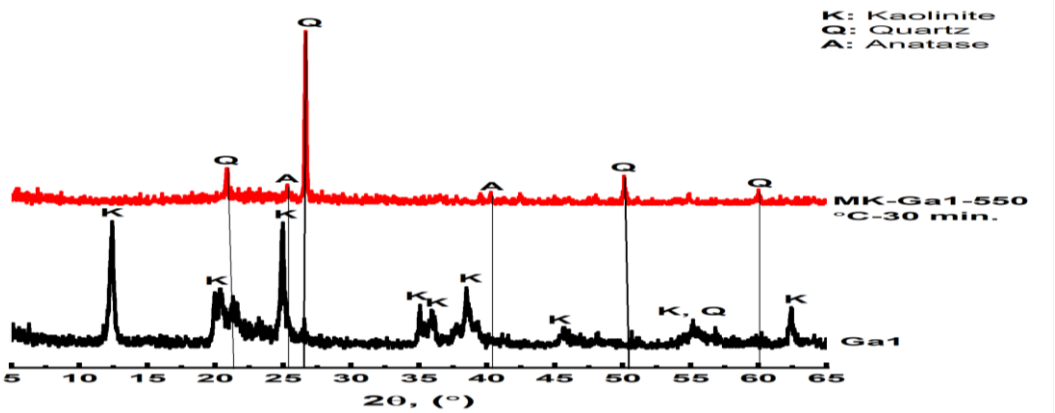

Fig. 10. XRD diffractograms of MK-Ga1 at 550 °C for 30mins.

3.2.3. Microstructure of MK

MK-Ga1 is represented by the irregular arrangement of the MK particles having broken edges (Figs. 11a and b). The ghost structure of the calcined kaolinite persisted and is represented by the preservation crystal aggregates of the platy pseudo-hexagonal kaolinite structure (Figs. 11a and b) [37, 56, 59, 61]. The elemental composition revealed from the microchemistry of MK-Ga1 confirms the presence of MK (Fig. 11) as reflected from the major recorded elemental concentration of Si and Al (65.16 and 34.84, respectively) (Point 1, Fig. 11b).

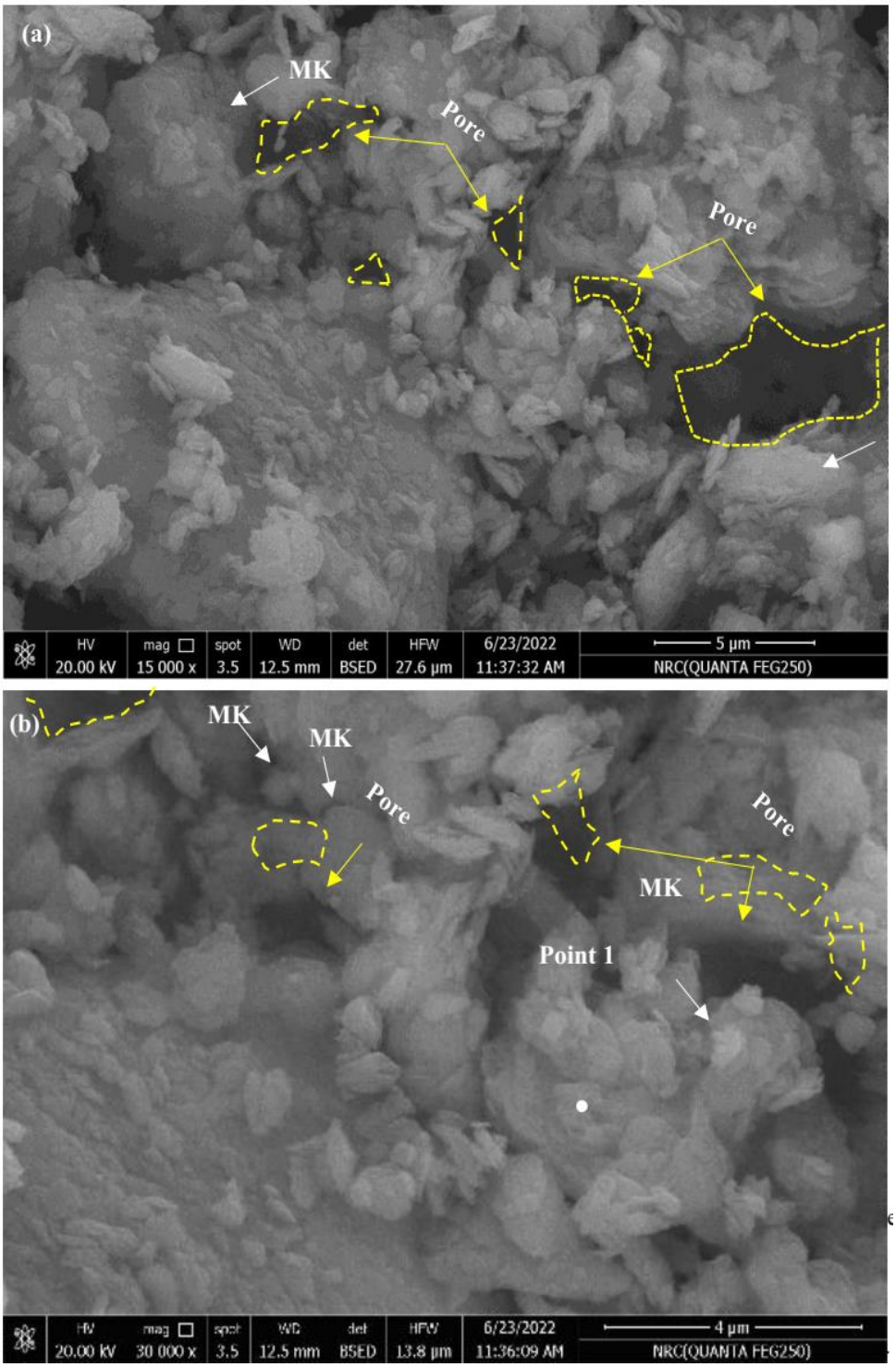

Fig. 11. SEM micrograph of MK-Ga1 at 550 °C for 30mins: (a) X15000 and (b) X30000 platy-pseudo-hexagonal particles with angular borders (MK, white arrows) and pore spaces (yellow dashed area).

3.2.4. MK Surface Area and Pore Volume

The BET analysis shows that the specific surface area of the Ga1 kaolin sample (4.47) is lower than that of the MK-Ga1 at 550°C for 30, 60 and 120 minutes (13.99, 13.11, 12.66m^2g^{-1}, respectively). However, the MK-Ga1 surface area decreases in the direction 30 > 60 > 120mins at 550°C (Fig. 12a) [63]. This is attributed mainly to the agglomeration of the MK particles due to sintering at higher temperatures [64]. The lower is the surface area, the fewer is the MK active sites available for pozzolanic reactions and, consequently, the lower is the MK-Ga1 pozzolanic activity with the soaking time (1732, 1136 and 386mg $Ca(OH)_2$/g MK, respectively) (Fig. 8a) [24, 70, 71].

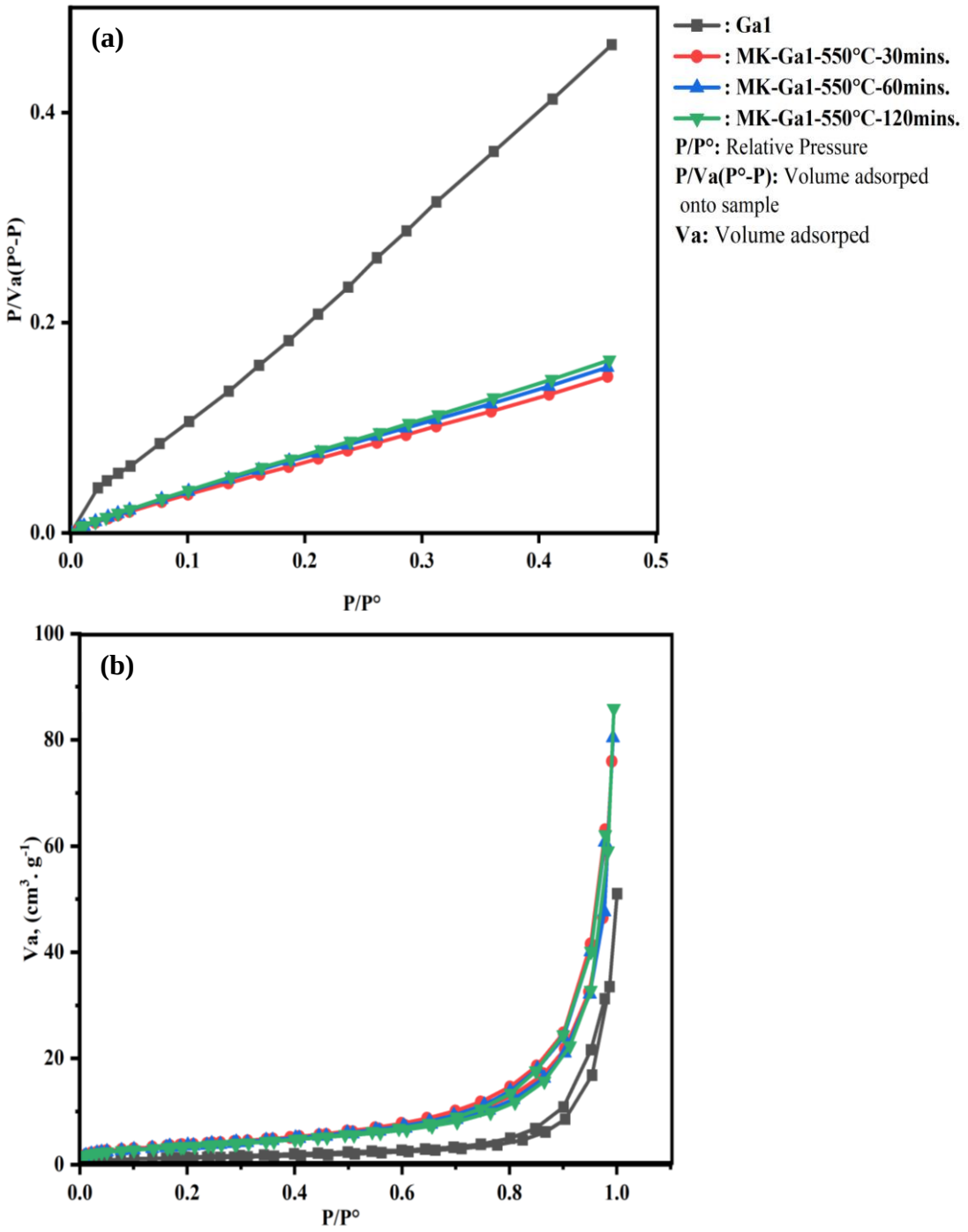

Fig. 12. (a) BET and (b) Isothermal plot of the Ga1 and MK-Ga1 samples heated at 550°C for 30, 60 and 120 minutes.

The isotherm of MK-Ga1 samples show the presence of type-II adsorption isotherm with H3 hysteresis loop as well as mesopores at the range 10-100nm (Fig. 12b) [72]. The pore volume, maximum pore diameter (dp_{max}) and average pore diameter (APD) of the MK-Ga1 sample heated at 550°C increased with soaking for 30, 60 and 120mins, respectively (0.116, 0.116, 0.117cm^3g^{-1}; 162.71, 209.98, 105.63nm and 21.81, 24.82, 30.72nm, respectively) (Table 3). The higher is the surface area (13.99m^2g^{-1}) (Table 3), the lower are the pore volume (0.116cm^3g^{-1}) and APD (21.81nm) (Table 3) and, consequently, the higher is the pozzolanic activity of MK-Ga1 at 550°C for 30mins (1732mg $Ca(OH)_2$/g MK, Fig. 8a). This is attributed to the fact that the smaller pores provide higher surface area per unit volume of the MK [63, 73].

The lower the APD, the higher is the nitrogen adsorption capacity (Vm) and, consequently, the higher is the surface area. Therefore, the MK-Ga1 heated at 550°C for 30mins represents the highest Vm value (3.21) as compared to those for the MK-Ga1 at 550°C for 60 and 120mins (3.01 and 2.91cm^3/g, respectively) (Table 3).

Table 3: Surface parameters of the MK samples heated at 550°C for 30, 60 and 120 minutes as calculated by the BET method

Locality	Sample code	Isotherm	BET surface area, (m^2/g)	Adsorption capacity, (Vm, cm^3/g)	Total pore volume, (cm^3/g)	BJH average pore diameter, (nm)	Max pore diameter, (dpmax, nm)	Pore type
El-Garf	Ga1	II	4.47	1.03	0.06	26.98	59.47	Meso
	MK-Ga1-550°C-30 mins.	II	13.99	3.21	0.12	21.81	162.71	Meso
	MK-Ga1-550°C-60 mins.	II	13.11	3.01	0.12	24.82	209.98	Meso
	MK-Ga1-550°C-120 mins.	II	12.66	2.91	0.12	30.72	105.63	Meso

Note* Ga1: Raw kaolin sample MK-Ga1: Metakaolin sample

4. Conclusion

This study investigates the transformation of raw kaolin into metakaolin (MK) through optimized calcination to save energy, increase production and the metakaolin marketing. By identifying the kaolin optimal calcination conditions, the research maximizes pozzolanic activity and highlights the key factors influencing it. These findings provide valuable insights for adding economic value to the kaolin raw materials. The key conclusions drawn from this study are as follows:

1. El-Garf kaolin samples are classified as coarse siltstones except for one sample (Ga3) which is composed of medium siltstone. The mineral composition of these samples (Ga1-Ga5) is composed of clay minerals (kaolinite) and non-clay minerals (quartz and anatase) as confirmed by XRD and FTIR.

2. The chemical composition of the kaolin samples is matched with the kaolinite/quartz ratio. The higher the degree of kaolinite ordering, the higher is the structural decomposition temperature. The mature microstructure of Ga1 kaolin is in conformity with its calculated high degree of ordering that demanded the maximum decomposition temperature at 580°C with maximum weight loss (13wt.%) among all the kaolin samples.

3. It is proved that 66% of the MK samples, i.e., 40 firing conditions, are highly pozzolanic and can be upscaled industrially. The optimum pozzolanic activity value (1732mg $Ca(OH)_2$/g MK) is for sample MK-Ga1 after calcination at 550°C for 30mins, whereas the minimum pozzolanic activity value (115mg $Ca(OH)_2$/g MK) is for sample MK-Ga5 after calcination at 750°C for 120mins.

4. The lower the kaolinite/quartz ratio as well as the higher total fluxes of the raw kaolin, the minimum is the MK pozzolanic activity.

5. The MK optimal surface area (13.99 m^2/g) is associated with low pore volume (0.116 cm^3/g) to enhance the MK pozzolanic activity. This is attributed to the fact that the smaller pores provide higher surface area per unit volume of the MK.

6. Future research will focus on large-scale industrial trials and explore additional activation techniques, such as grinding and chemical, to further enhance the material's properties.

5. Conflicts of Interest

"There are no conflicts to declare".

6. Formatting of Funding Sources
The research leading to these results received funding from the Academy of Scientific Research and Technology [ASRT] under Grant Agreement No [4357].

7. Acknowledgments
This work is financially supported by the Academy of Scientific Research and Technology [ASRT], Egypt, [Project No. 4357]. Thank the ASRT for financial support. All facilities provided by the Applied Mineralogy Laboratory, Faculty of Science, Ain Shams University are greatly appreciated.

8. References

[1] Ekosse, GIE (2010) Kaolin deposits and occurrences in Africa: Geology, mineralogy and utilization. Applied Clay Science 50(2): 212–236. https://doi.org/10.1016/j.clay.2010.08.003
[2] Taib, M (2015) The Mineral Industry of Egypt 2015. https://www.researchgate.net/publication/334042121
[3] Virta, RL (2015) Clay and shale (Advanced Release) in 2013: Minerals_Yearbook. U.S. Geological Survey 1:22. Available at: http://minerals.usgs.gov/minerals/pubs/ myb.html (web archive link, 07 February 2018), Accessed date: 7 February
[4] Boulis, SN & Attia, AKM (1994) Mineralogical and chemical composition of Carboniferous and Cretaceous kaolins from a number of localities in Egypt. Mineral Soc Egypt 100: 99–127.
[5] El-Kammar, A, Abu-Zied, HT, Galal, M & Osman, D (2017) Composition, radioactivity, and possible applications of kaolin deposits of Sinai, Egypt. Arabian Journal of Geosciences 10(21). https://doi.org/10.1007/s12517-017-3223-6
[6] Awad, ME, Amer, R, López-Galindo, A, El-Rahmany, MM, García del Moral, LF & Viseras, C (2018) Hyperspectral remote sensing for mapping and detection of Egyptian kaolin quality. Applied Clay Science 160: 249–262. https://doi.org/10.1016/j.clay.2018.02.042
[7] Sharaka, HK, El-Desoky, HM, Abd El Moghny, MW, Abdel Hafez, NA & Saad, SAA (2022) Mineralogy and lithogeochemistry of lower Cretaceous kaolin deposits in the Malha Formation, Southwestern Sinai, Egypt: Implications for the building and construction industry. Journal of Asian Earth Sciences X: 7. https://doi.org/10.1016/j.jaesx.2022.100087
[8] El-Desoky, HM, Abd El Moghny, MW, Abdel Hafez, NA, El-Shahat, OR, Farouk, S & Sharaka, HK (2022) Geochemical Parameters for Evaluating the Aptian-Albian Kaolin Deposits at Abu Darag Region, Gulf of Suez: Implications for the Paleoclimatic Conditions in the Depositional Environments. Iraqi National Journal of Earth Science 22(2): 67–89. https://doi.org/10.33899/earth.2022.135180.1025
[9] Abdelhalim, A, Melegy, A & Othman, D (2023) Implication of Lower Cretaceous Kaolinitic Clay Deposits Characterization in Industry, Case: West Central Sinai, Egypt. Egyptian Journal of Chemistry, 66(5): 129–150. https://doi.org/10.21608/EJCHEM.2022.153794.6670
[10] Razek, A (1994) processing trials on kaolin-bearing sandstone from the Gulf of Aqaba and Abu Zeneima areas, southern Sinai, Egypt. Geological Survey of Egypt, 1st International symposium on industrial application of clays: 78–88.
[11] Abdel-Khalek, NA (1999) The Egyptian kaolin: an outlook in the view of the new climate of investment. In Applied Clay Science (15): 325-336. https://doi.org/10.1016/S0169-1317(99)00026-5
[12] Panesar, DK (2019) Supplementary cementing materials. In Developments in the Formulation and Reinforcement of Concrete, Elsevier: 55–85. https://doi.org/10.1016/B978-0-08-102616-8.00003-4
[13] Apeh, AJ (2022) Hydration Behaviour and Characteristics of Binary Blended Metakaolin Cement Pastes. Journal of Building Materials and Structures 9(1): 57–73. https://doi.org/10.34118/jbms.v9i1.1606
[14] Moya, JS, Cabal, B, Lopez-Esteban, S, Bartolomé, JF & Sanz, J (2024) Significance of the formation of pentahedral aluminum in the reactivity of calcined kaolin/metakaolin and its applications. In Ceramics International, Elsevier 50 (1): 1329–1340. https://doi.org/10.1016/j.ceramint.2023.10.304
[15] Mitrović, AA (2011) Pozzolan obtained by mechanochemical treatment of kaolinite clay. AIP Conference Proceedings 1400: 82–86. https://doi.org/10.1063/1.3663090
[16] Caballero, LR, Paiva, MDDM, Fairbairn, EDMR & Filho, RDT (2019) Thermal, mechanical and microstructural analysis of metakaolin based geopolymers. Materials Research 22(2). https://doi.org/10.1590/1980-5373-MR-2018-0716
[17] Moodi, F, Ramezanianpour, AA & Safavizadeh, AS (2011) Evaluation of the optimal process of thermal activation of kaolins. Scientia Iranica 18(4 A): 906–912. https://doi.org/10.1016/j.scient.2011.07.011
[18] Ambroise, J, Murat, M & Péra, J (1985) Hydration reaction and hardening of calcined clays and related minerals V. Extension of the research and general conclusions. Cement and Concrete Research 15(2): 261–268. https://doi.org/10.1016/0008-8846(85)90037-7
[19] Almenares, RS, Vizcaíno, LM, Damas, S, Mathieu, A, Alujas, A & Martirena, F (2017) Industrial calcination of kaolinitic clays to make reactive pozzolans. Case Studies in Construction Materials (6): 225–232. https://doi.org/10.1016/j.cscm.2017.03.005
[20] Barnes, P & Bensted, J (2002) Structure and Performance of Cements (2nd ed.).
[21] Shafiq, N, Nuruddin, MF, Khan, SU & Ayub, T (2015) Calcined kaolin as cement replacing material and its use in high strength concrete. Construction and Building Materials 81: 313–323. https://doi.org/10.1016/j.conbuildmat.2015.02.050
[22] Hollanders, S, Adriaens, R, Skibsted, J, Cizer, Ö & Elsen, J (2016) Pozzolanic reactivity of pure calcined clays. Applied Clay Science 132–133, 552–560. https://doi.org/10.1016/j.clay.2016.08.003

[23] Kassa, AE, Shibeshi, NT, Tizazu, BZ & Prabhu, SV (2022) Characteristic Investigations on Ethiopian Kaolinite: Effect of Calcination Temperature on] Pozzolanic Activity and Specific Surface Area. Advances in Materials Science and Engineering. https://doi.org/10.1155/2022/2481066

[24] Onyelowe, KC, Naghizadeh, A, Aneke, FI, Kontoni, DPN, Onyia, ME, Welman-Purchase, M, Ebid, AM, Adah, EI & Stephen, LU (2023) Characterization of net-zero pozzolanic potential of thermally-derived metakaolin samples for sustainable carbon neutrality construction. Scientific Reports 13(1). https://doi.org/10.1038/s41598-023-46362-y

[25] Murat, M & Comel, C (1983) Hydration reaction and hardening of calcined clays and related minerals. iii. influence of calcination process of kaolinite on mechanical strengths of hardened metakaolinite. In cement and concrete research 13 (5): 631-637. https://doi.org/10.1016/0008-8846(83)90052-2

[26] Granizo, ML, Blanco-Varela, MT & Palomo, A (2000) Influence of the starting kaolin on alkali-activated materials based on metakaolin. Study of the reaction parameters by isothermal conduction calorimetry. Journal of materials science 35: 6309– 6315.

[27] Kakali, G, Perraki, T, Tsivilis, S & Badogiannis, E (2001) Thermal treatment of kaolin: the effect of mineralogy on the pozzolanic activity. In Applied Clay Science 20: 73-80. www.elsevier.comrlocaterclay https://doi.org/10.1016/S0169-1317(01)00040-0

[28] Tironi, A, Trezza, MA, Irassar, EF & Scian, AN (2012) Thermal Treatment of Kaolin: Effect on the Pozzolanic Activity. Procedia Materials Science 1: 343–350. https://doi.org/10.1016/j.mspro.2012.06.046

[29] Krishnan, S & Bishnoi, S (2015) High level clinker replacement in ternary limestone-calcined clay-clinker cement. In Advances in Structural Engineering: Materials, three (Springer India.): 1725–1731.

[30] Irland HA (1971) Insoluble residues (Carver RE: procedures in sedimentary petrology, Ed.). Willley-Intersciences.

[31] Jackson, ML, Whitting, LD & Pennington, RP (1950) Segregation procedures for mineralogical analysis of soils. Soil Sci. Soc. Am. Proc. 14: 77–81.

[32] Leith, CJ (1950) Removal of iron oxide coatings from mineral grains. Journal of Sedimentary Research 20(3): 174–176. https://doi.org/10.1306/D42693DC-2B26-11D7-8648000102C1865D

[33] Ilić, BR, Mitrović, AA & Miličić, LR (2010) Thermal treatment of kaolin clay to obtain metakaolin. Hemijska Industrija 64(4): 351–356. https://doi.org/10.2298/HEMIND100322014I

[34] Balczár, I, Korim, T, Kovács, A & Makó, E (2016) Mechanochemical and thermal activation of kaolin for manufacturing geopolymer mortars – Comparative study. Ceramics International 42(14): 15367–15375. https://doi.org/10.1016/j.ceramint.2016.06.182

[35] Madejová, J, Gates, WP & Petit, S (2017) IR Spectra of Clay Minerals. In Developments in Clay Science 8: 107–149. https://doi.org/10.1016/B978-0-08-100355-8.00005-9

[36] Jozanikohan, G & Abarghooei, MN (2022) The Fourier transform infrared spectroscopy (FTIR) analysis for the clay mineralogy studies in a clastic reservoir. Journal of Petroleum Exploration and Production Technology 12(8): 2093–2106. https://doi.org/10.1007/s13202-021-01449-y

[37] Liew, YM, Kamarudin, H, Mustafa Al Bakri, AM, Luqman, M, Khairul Nizar, I, Ruzaidi, CM & Heah, CY (2012) Processing and characterization of calcined kaolin cement powder. Construction and Building Materials 30: 794–802. https://doi.org/10.1016/j.conbuildmat.2011.12.079

[38] Pongpiachan, S (2014) FTIR Spectra of Organic Functional Group Compositions in PM2.5 Collected at Chiang-Mai City, Thailand during the Haze Episode in March 2012, journal of applied sciences 14 (22): 2967-2977. https://ui.adsabs.harvard.edu/link_gateway/2014JApSc.14.2967P/doi:10.3923/jas.2014.2967.2977

[39] Nandiyanto, ABD, Oktiani, R & Ragadhita, R (2019) How to read and interpret ftir spectroscope of organic material. Indonesian Journal of Science and Technology 4(1): 97–118. https://doi.org/10.17509/ijost.v4i1.15806

[40] Silverstein, RM, Bassler, GC, Morrill, TC (1981) Spectrometric Identification of Organic Compmmds. In: 4th Edn JW and S (ed). New York, USA.

[41] Salem, MAA (1990) Comparative petrological and mineralogical studies on the kaolin bearing successions in west central Sinai with emphasis on industrial applications.

[42] Liu, Z, Wang, A, Zhang, Q, Liu, J, Ma, H, Li, D & Xing, L (2021) Visible-light-driven photocatalytic activity of kaolinite: Sensitized by in situ growth of Cu-TiO2. Environmental Progress and Sustainable Energy 40(1): 1-10. https://doi.org/10.1002/ep.13479

[43] Li, X, Peng, K, Chen, H & Wang, Z (2018) TiO2 nanoparticles assembled on kaolinites with different morphologies for efficient photocatalytic performance. Scientific Reports 8(1). https://doi.org/10.1038/s41598-018-29563-8

[44] Aly, GM (2005) Mineralogy, geochemistry and economic evaluation of some kaolin occurrences in Egypt. PHD Thesis, Faculty of science, Tanta university, Egypt.

[45] Shoval, S, Panczer, G & Boudeulle, M (2008) Study of the occurrence of titanium in kaolinites by micro-Raman spectroscopy. Optical Materials 30(11): 1699–1705. https://doi.org/10.1016/j.optmat.2007.11.012

[46] Liu, L, Liu, Q, Algeo, T, Zhang, H, Yang, Y, Peng, G, Zhang, S, Hong, H & Liu, D (2021) Mineralogy, Geochemistry, and Genesis of Kaolinitic Claystone Deposits in the Datong Coalfield, Northern China. Clays and Clay Minerals 69(1): 68–93. https://doi.org/10.1007/s42860-020-00109-2

[47] Földvári, M (2011) Handbook of thermogravimetric system of minerals and its use in geological practice. Geological Institute of Hungary.

[48] Ayalew, AA (2020) Development of Kaolin Clay as a Cost-Effective Technology for Defluoridation of Groundwater. International Journal of Chemical Engineering:1-10. https://doi.org/10.1155/2020/8820727

[49] Sperinck, S, Raiteri, P, Marks, N & Wright, K (2011) Dehydroxylation of kaolinite to metakaolin - A molecular dynamics study. Journal of Materials Chemistry 21(7): 2118–2125. https://doi.org/10.1039/c0jm01748e
[50] Wang, H, Li, C, Peng, Z & Zhang, S (2011) Characterization and thermal behavior of kaolin. Journal of Thermal Analysis and Calorimetry 105(1): 157–160. https://doi.org/10.1007/s10973-011-1385-0
[51] White, CE, Provis, JL, Proffen, T, Riley, DP & van Deventer, JSJ (2010) Density functional modeling of the local structure of kaolinite subjected to thermal dehydroxylation. J. Phys. Chem. A (114): 4988–4996.
[52] Smykatz-Kloss, W (1974) Differential Thermal Analysis: applications and results in mineralogy. Spinger Verlag, Berlin – Heidelberg – New York, 185.
[53] Wenxiu Rao, Xin Liu, Guocheng Lv, Meng Liu, Lijuan Wang, Jinan Niu, Zhaohui Li, & Libing Liao (2024) Correlation between Hinckley index and stacking order-disorder in kaolinite. American Mineralogist 109(1): 135–143. https://doi.org/10.2138/am-2022-8830
[54] Murray, HH (2000) Traditional and new applications for kaolin, smectite, and palygorskite: a general overview. In Applied Clay Science 17: 207-221. www.elsevier.nlrlocaterclay. https://doi.org/10.1016/S0169-1317(00)00016-8
[55] San Cristóbal, AG, Castelló, R, Martín Luengo, MA & Vizcayno, C (2010) Zeolites prepared from calcined and mechanically modified kaolins. A comparative study. Applied Clay Science 49(3): 239–246. https://doi.org/10.1016/j.clay.2010.05.012
[56] Rashad, AM (2013) Metakaolin as cementitious material: History, scours, production and composition-A comprehensive overview. In Construction and Building Materials 41: 303–318. https://doi.org/10.1016/j.conbuildmat.2012.12.001
[57] Mitrović, A & Zdujić, M (2014) Preparation of pozzolanic addition by mechanical treatment of kaolin clay. International Journal of Mineral Processing 132: 59–66. https://doi.org/10.1016/j.minpro.2014.09.004
[58] Ferraz, E, Andrejkovičová, S, Hajjaji, W, Velosa, AL, Silva, AS & Rocha, F (2015) Pozzolanic activity of metakaolins by the French standard of the modified Chapelle test: A direct methodology. Acta Geodynamica et Geomaterialia 12(3): 289–298. https://doi.org/10.13168/AGG.2015.0026
[59] Mehsas, B, Siline, M & Zeghichi, L (2021) Development of supplementary cementitious materials from Algerian kaolin: elaboration of metakaolin and assessment of pozzolanicity. Innovative Infrastructure Solutions 6(2): 2-12. https://doi.org/10.1007/s41062-020-00444-2
[60] Alvarez-Coscojuela, A, Mañosa, J, Formosa, J & Chimenos, JM (2024) Structural characterisation and reactivity measurement of chemically activated kaolinite. Journal of Building Engineering 87: 1-15. https://doi.org/10.1016/j.jobe.2024.109051
[61] Liu, Y, Lei, S, Lin, M, Li, Y, Ye, Z & Fan, Y (2017) Assessment of pozzolanic activity of calcined coal-series kaolin. Applied Clay Science 143: 159–167. https://doi.org/10.1016/j.clay.2017.03.038
[62] Ilić, B, Radonjanin, V, Malešev, M, Zdujić, M & Mitrović, A (2016) Effects of mechanical and thermal activation on pozzolanic activity of kaolin containing mica. Applied Clay Science 123: 173–181. https://doi.org/10.1016/j.clay.2016.01.029
[63] Hollanders, S (2017) Mineralogical study of the pozzolanic properties of calcined clays, PHD, KU Leuven, Science, Engineering & Technology.
[64] Fitos, M, Badogiannis, EG, Tsivilis, SG & Perraki, M (2015) Pozzolanic activity of thermally and mechanically treated kaolins of hydrothermal origin. Applied Clay Science 116–117, 182–192. https://doi.org/10.1016/j.clay.2015.08.028
[65] Mackenzie, RC (1970) Differential Thermal Analysis. http://pascal-francis.inist.fr/vibad/index.php?action=getRecordDetail&idt=PASCALGEODEBRGM732202496
[66] Sanz, J, Mandani, A, Serratosa, JM, Moya, JS & Aza, S (1988) Aluminum−27 and silicon−29 magic-angle spinning nuclear magnetic resonance study of the kaolinite mullite transformation. Journal of the American Ceramic Society 71: 418–421.https://doi.org/10.1111/j.1151-2916.1988.tb07513.x
[67] Khatib, JM, Baalbaki, O & ElKordi, AA (2018) Metakaolin. In Waste and Supplementary Cementitious Materials in Concrete: Characterisation, Properties and Applications 493–511. Elsevier. https://doi.org/10.1016/B978-0-08-102156-9.00015-8
[68] Khaled, Z, Mohsen, A, Soltan, AM & Kohail, M (2023) Optimization of kaolin into Metakaolin: Calcination Conditions, mix design and curing temperature to develop alkali activated binder. Ain Shams Engineering Journal 14(6): 1-14. https://doi.org/10.1016/j.asej.2023.102142
[69] Dhar, M & Bishnoi, S (2024) Influence of calcination temperature on the physical and chemical characteristics of kaolinitic clays for use as supplementary cementitious materials. Cement and Concrete Research 178, 107464. https://doi.org/10.1016/j.cemconres.2024.107464
[70] Silva Neto, JA, Marçal, NA, Nóbrega, AF, Nóbrega, ACV, Souza, JJN & Malheiro, R (2024) Use of metakaolin with a low surface area and rich in quartz and iron as a precursor in the production of structural alkali-activated concrete. Construction and Building Materials 430:136418. https://doi.org/10.1016/j.conbuildmat.2024.136418
[71] Acevedo, NIA, Rocha, MCG & Bertolino, LC (2017) Mineralogical characterization of natural clays from Brazilian Southeast region for industrial applications. Ceramica 63(366):253–262. https://doi.org/10.1590/0366-69132017633662045
[72] Li, J, Mailhiot, S, Alzeer, MIM, Luukkonen, T, Kantola, AM, Telkki, VV & Kinnunen, P (2024) Impact of NH4OH treatment on the ion exchange and pore characteristics of a metakaolin-based geopolymer. RSC Advances 14(28): 19935–19944. https://doi.org/10.1039/d4ra03972f

[73] Wang, FL, & Huang, PM (2001) Effects of organic matter on the rate of potassium adsorption by soils. Canadian Journal of Soil Science, 81(3 SPEC. ISS.), 325–330. https://doi.org/10.4141/S00-069

[74] Zunino, F & Scrivener, K (2024) Reactivity of kaolinitic clays calcined in the 650 °C–1050 °C temperature range: Towards a robust assessment of overcalcination. Cement and Concrete Composites, 146, 105380. https://doi.org/10.1016/j.cemconcomp.2023.105380

[75] Eldin, HS, Abdullah, NA & Ismail, MF (2022) Preparation of meta phase of kaolinite as a precursor for geopolymer adsorbent fabrication. Epitoanyag-Journal of Silicate Based and Composite Materials, 74, 82-87.https://doi.org/10.14382/epitoanyag-jsbcm.2022.13

[76] NF P18-513 (2010), Metakaolin. Pozzolanic addition for concrete. Definitions, specifications and conformity criteria. Association Française de Normalisation, La Plaine Saint-Denis, (in French).